A&A manuscript no.
(will be inserted by hand later)

Your thesaurus codes are:
06 (05.05.1; 08.02.3; 08.09.2 Cyg X–3; 13.07.2; 13.09.6; 13.25.5)

ASTRONOMY AND ASTROPHYSICS
15.3.1996

Hard X-ray and IR observations of Cygnus X–3

S. M. Matz[1], **R. P. Fender**[2], **S. J. Bell Burnell**[2], **J. E. Grove**[3], and **M. S. Strickman**[3]

[1] Department of Physics and Astronomy, Northwestern University, Dearborn Observatory, Evanston, Illinois 60208-2900 USA, Internet: s-matz@nwu.edu
[2] Dept. of Physics, The Open University, Walton Hall, Milton Keynes MK7 6AA U.K.
[3] Naval Research Lab, Code 7650, Washington, D.C. 20375 USA

March 15, 1996

Abstract. In 1994 June–July we obtained nearly concurrent measurements of Cyg X–3 in hard X-rays and the infrared, using the OSSE instrument on GRO and the UKIRT. OSSE made a high significance measurement of the hard X-ray (> 50 keV) orbital light curve. Five days after the end of the OSSE observations we obtained a good IR K-band light curve from data covering one orbit of Cyg X–3. Measurements of the light curve phase and shape probe the geometry of the system and the physics of radiation production and scattering. We determined for the first time that the light curve *phases* are consistent at these two different wavelengths. The light curve *shapes* were both marginally *inconsistent* (at about the 0.2% level) with the canonical soft X-ray shape measured by EXOSAT in 1983–1985. Underlying variations in DC IR flux and flaring during the observation make it difficult to draw unambiguous conclusions; more observations, with better IR coverage, are needed.

Key words: X-ray binaries – Cygnus X–3 – X-rays – Infrared

1. Introduction

One of the mysteries associated with the bright X-ray source Cyg X–3 is the change in the ~ 4.8 hr period. The period, commonly thought to correspond to the orbital cycle of a compact object/companion star system, is increasing, with $\dot{P}/P \sim 10^{-6}$ yr^{-1} (e.g., Kitamoto et al. 1992). This is inconsistent with the Roche lobe transfer of material from a main sequence star to the compact object (Molnar 1988). It can be explained, under certain conditions, by a wind from the companion star (van Kerkwijk et al. 1992). The period is typical of low-mass X-ray binaries; however, there is evidence that the companion is actually a high-mass Wolf-Rayet star (van Kerkwijk et al. 1992). There is also a significant (4σ) $\ddot{P}$ term in the ephemeris, first measured by Van der Klis and Bonnet-Bidaud (1989).

The orbital light curve, observed in IR and X-rays, is asymmetric. This requires some asymmetry in the system, either in the binary orbit itself (i.e., a significant eccentricity) or in the matter in the system. If the asymmetry is caused by an elliptical orbit, the light curve shape is expected to change significantly over time due to apsidal motion (periastron advance) (Ghosh et al. 1981). If the orbit is elliptical, apsidal motion may also be responsible for some or all of the apparent period increase (Elsner et al. 1980). Therefore, measurements of the light curve shape are directly related to the orbital dynamics. Short-term variations in the light curve shape, however, complicate the interpretation of individual observations (e.g., van der Klis & Bonnet-Bidaud 1981).

The asymmetric, non-eclipsing light curve, along with the observed He lines in the IR spectrum (van Kerkwijk et al. 1992) imply that the primary source is surrounded by dense material. This material may be in the form of a wind from the secondary (Pringle 1974; Willingale, King, & Pounds 1985), a "cocoon" (Milgrom & Pines 1978), or an accretion disk corona (White & Holt 1982). See Bonnet-Bidaud & Chardin (1988) for a valuable review of many of the Cyg X–3 observations and theories.

It has been theorized that Cyg X–3 shows so many unique properties because it is in a very short-lived, transitional phase of binary evolution. If this is the case a study of its dynamics (via the orbital ephemeris), and local environment (via the light curve and spectrum) may have broad implications for X-ray binaries in general.

2. Observation Summary

2.1. OSSE

The OSSE instrument on GRO is described in detail by Johnson et al. (1993). It consists of four independent cylindrical NaI/CsI phoswhich scintillators, actively shielded

Send offprint requests to: S. M. Matz

Report Documentation Page					*Form Approved* *OMB No. 0704-0188*
Public reporting burden for the collection of information is estimated to average 1 hour per response, including the time for reviewing instructions, searching existing data sources, gathering and maintaining the data needed, and completing and reviewing the collection of information. Send comments regarding this burden estimate or any other aspect of this collection of information, including suggestions for reducing this burden, to Washington Headquarters Services, Directorate for Information Operations and Reports, 1215 Jefferson Davis Highway, Suite 1204, Arlington VA 22202-4302. Respondents should be aware that notwithstanding any other provision of law, no person shall be subject to a penalty for failing to comply with a collection of information if it does not display a currently valid OMB control number.					
1. REPORT DATE **1996**		2. REPORT TYPE			3. DATES COVERED **00-00-1996 to 00-00-1996**
4. TITLE AND SUBTITLE **Hard X-ray and IR observations of Cygnus X-3**					5a. CONTRACT NUMBER
					5b. GRANT NUMBER
					5c. PROGRAM ELEMENT NUMBER
6. AUTHOR(S)					5d. PROJECT NUMBER
					5e. TASK NUMBER
					5f. WORK UNIT NUMBER
7. PERFORMING ORGANIZATION NAME(S) AND ADDRESS(ES) **Naval Research Laboratory,Code 7650,4555 Overlook Avenue, SW,Washington,DC,20375**					8. PERFORMING ORGANIZATION REPORT NUMBER
9. SPONSORING/MONITORING AGENCY NAME(S) AND ADDRESS(ES)					10. SPONSOR/MONITOR’S ACRONYM(S)
					11. SPONSOR/MONITOR’S REPORT NUMBER(S)
12. DISTRIBUTION/AVAILABILITY STATEMENT **Approved for public release; distribution unlimited**					
13. SUPPLEMENTARY NOTES					
14. ABSTRACT					
15. SUBJECT TERMS					
16. SECURITY CLASSIFICATION OF:			17. LIMITATION OF ABSTRACT	18. NUMBER OF PAGES **4**	19a. NAME OF RESPONSIBLE PERSON
a. REPORT **unclassified**	b. ABSTRACT **unclassified**	c. THIS PAGE **unclassified**			

Standard Form 298 (Rev. 8-98)
Prescribed by ANSI Std Z39-18

on the sides by NaI. The normal spectral energy range is 50 keV to 10 MeV. The front of each detector is covered by a tungsten collimator, which defines a rectangular ($11.4^\circ \times 3.8^\circ$ FWHM) field of view. Each detector may be positioned independently about an axis parallel to the long direction of the collimator. Spectral data are accumulated in two-minute intervals, alternating between source and background pointings of the detectors. In the Cyg X–3 observations the orientation of the spacecraft and the positions of the detector pointings were chosen so that there was no significant flux contribution from Cyg X–1 in either the source or the background.

OSSE made seven significant observations of Cyg X–3 from 1991 to 1994: 1991 May 30 – Jun 15 (viewing period 2), 1991 Aug 8 – 15 (VP 7), 1991 Nov 28 – Dec 11 (VP 15), 1992 Dec 9 – 15 (VP 203), 1994 May 24 – 31 (VP 328), 1994 June 7 – 17 (VP 330–331), and 1994 July 7 – 12 (VP 333). OSSE has detected significant flux from Cyg X–3 up to $\sim$ 200 keV. Some results of the earlier observations have been described by Matz et al. (1994). We focus here on the measurements of Cyg X–3 taken during 1994 June 7–17 and July 7–12 (TJD 9510–9520 and 9540–9545).

2.2. UKIRT

Cyg X–3 was observed with the UK Infrared Telescope (UKIRT) on the night of 1994 July 17 UT (TJD 9550) over nearly one entire 4.8 hr orbital cycle, using the IRCAM3 instrument. IRCAM3 is a 256 × 256 imaging array, operating in the 1–5 micron range, with a resolution of 0.286 arcsec/pixel. The source was monitored in the J (1.2 micron), H (1.6 micron), K (2.2 micron) and nbL (3.6 micron) bands. Weather conditions were not good but seeing was reasonable and nearby field stars allowed accurate relative photometry to be performed. Faint standard G93-48 was used for absolute flux calibration at J, H, and K. A comparison of variability in all four bands will be discussed elsewhere. Mosaicing of images revealed at least ten previously undetected objects within a few arcsec of Cyg X–3 — see Fender & Bell Burnell (1995) for a new K-band finder chart.

3. OSSE Ephemeris Derivation

The data in this paper were analysed using an up-to-date X-ray ephemeris derived from previous observations (see Kitamoto et al. (1992) and references therein), the last of which was in 1987, plus the seven OSSE observations from 1991 to 1994.

For each of the seven OSSE observations of Cyg X–3 the two-minute background-subtracted count rate spectra were integrated over the energy range 44–130 keV. The time of each two-minute observation was corrected to the solar system barycenter. The orbital phase was then calculated; as a test of ephemeris dependence, three different methods were used: a constant period (0.19969079d) and

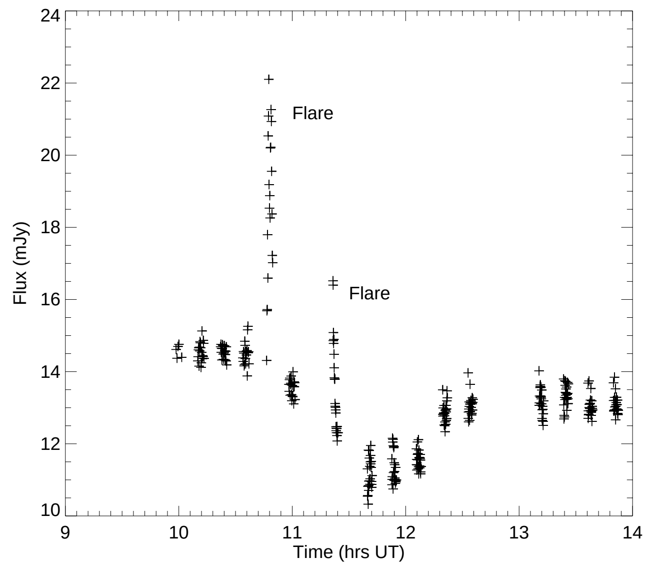

Fig. 1. UKIRT corrected K-band data from July 17, 1994. Individual points represent 10 s accumulations. Error bars are roughly consistent with the symbol size.

the quadratic and cubic ephemerides of van der Klis & Bonnet-Bidaud (1989). Orbital light curves were produced by accumulating the data into the appropriate phase bins. Due to the relatively weak flux from Cyg X–3 at hard X-ray energies, the OSSE data must be epoch-folded over a number of days to produce a significant signal. This has the advantage of averaging over the known cycle-to-cycle variations in the light curve shape. A significant orbital modulation of the flux was observed in each of the seven viewing periods except VP 203, where the fitted light curve amplitude was only marginally positive ($\sim 2.8\sigma$ above zero).

The EXOSAT template light curve (van der Klis & Bonnet-Bidaud 1989) was fit to the OSSE light curve for each observation, allowing the phase, amplitude, and background (DC) level to vary. In all cases except for VP 333 the X-ray light curve template provided a statistically acceptable fit to the OSSE data; in VP 333 the χ^2 was high (58 for 29 dof) but the template seemed to describe the data well enough to determine the phase. The template is better than the alternative model, a simple sine function, which has commonly been used to fit the X-ray data to determine pulse arrival times even though it is not a good description of the average X-ray light curve shape.

For each of the light curves, the shift of the fitted template from phase 0 as predicted by the ephemerides was used to calculate a pulse arrival time for a cycle near the center of the observation. The pulse arrival time is equal to the predicted arrival time corrected by the fitted difference in phase multiplied by the period. There are no significant differences between the pulse arrival times derived using the quadratic, cubic, and constant period ephemerides. The OSSE arrival times are consistent (within errors) with extrapolations of the ephemerides of

Kitamoto et al. (1992) and van der Klis & Bonnet-Bidaud (1989).

We then derived a new ephemeris by combining the OSSE arrival times with the earlier soft X-ray results. Consistent with previous fits (e.g., van der Klis & Bonnet-Bidaud 1989; Kitamoto et al. 1992), we can exclude a simple quadratic ephemeris (at a confidence level of 10^{-11} or better), while a cubic description (with a non-zero $\ddot{P}$) does fit the data.

The preliminary results are shown in Table 1, with parameters defined as in van der Klis & Bonnet-Bidaud (1989). T_n is the arrival time of the minimum of the nth orbital cycle. The numbers in the final OSSE ephemeris may change slightly with refinements in the phase determination.

Table 1. PRELIMINARY Best-Fit Cubic Ephemeris

$$(T_n = T_0 + P_0 n + c_0 n^2 + dn^3)$$

Parameter	Fitted value
T_0	2440949.8999 ± 0.0014 HJD
P_0	$0.19968240 \pm (2.8 \times 10^{-7})$ d
c_0	$(1.81 \pm 0.16) \times 10^{-10}$ d
d	$(-2.04 \pm 0.25) \times 10^{-15}$ d
χ^2 (dof)	114.68 (84)
Conf. level	0.015

4. Orbital light curve analysis

To produce the orbital IR and X-ray light curves for the 1994 June–July observations, the two flaring periods (Fig. 1) were first removed from the IR data. The data were then corrected to the solar system barycenter (SSB) and epoch-folded using orbital phases calculated from the OSSE cubic ephemeris shown in Table 1. For comparison, the IR and OSSE data were binned at same time resolution. The plotted errors in the IR data are not the statistical errors of the individual measurements, but the observed variance of the data included in each phase bin. The size of these variances reflect real source fluctuations, as determined from relative photometry referenced to nearby stars Z and D.

The resulting light curves were fitted with the EXOSAT soft X-ray template (van der Klis & Bonnet-Bidaud 1989) in the manner described above. The phase and amplitude of the template, and the DC background intensity were varied to minimize χ^2 for the X-ray and IR data independently. Figure 2 shows the resulting light curves with best-fit X-ray template (dashed line) overplotted. The gaps in the IR light curve correspond to gaps in the data collection. From the fits we can determine, for each of the two data sets, the phase of the minimum and the

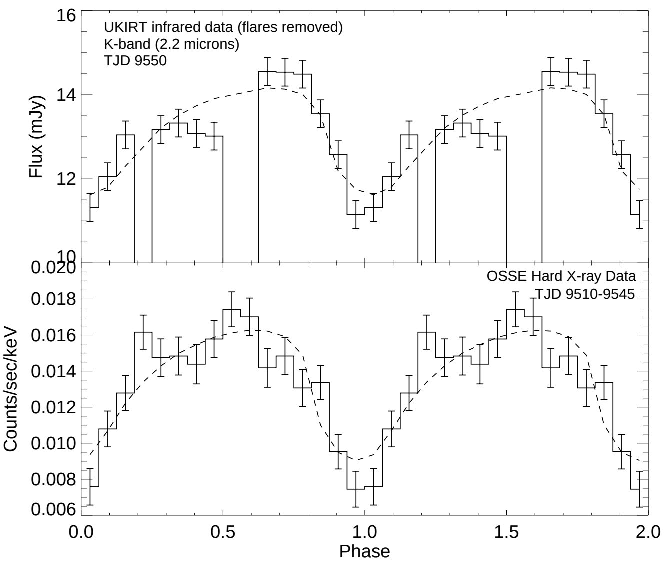

Fig. 2. OSSE and UKIRT light curves with best-fit X-ray template overplotted (dashed line). Two cycles are shown.

consistency of the measured shape with the soft X-ray template.

5. Results

5.1. Light curve phase

The fitted OSSE phase is 0.016 ± 0.022 and the IR phase is 0.069 ± 0.024. The hard X-ray and IR light curves are consistent with the same phase at minimum within 1.6σ. Mason, Córdova, & White (1986) found that the IR and soft X-ray light curves had the same phase. The consistency of the hard X-ray and IR phases thus justifies combining the hard X-ray data with earlier soft X-ray observations to extend the ephemerides.

Some caution needs to be exercised in interpreting this result. Cyg X–3 is known to have significant cycle-to-cycle variations in the light curve shape. Here we are comparing one IR cycle (incompletely sampled, and with possible underlying variations) to the OSSE multi-orbit average.

5.2. Light curve shape

Previous observations showed that the IR and soft X-ray light curves had the same shape (Mason, Córdova, & White 1986). However, here both the OSSE and IR light curves are marginally *inconsistent* (at about the 0.2% level) with the canonical soft X-ray template (van der Klis & Bonnet-Bidaud 1989). Again, we cannot rule out that the difference in IR light curve shape was caused by underlying DC variations during the measured cycle or by the normal cycle-to-cycle differences. In fact, a short period of UKIRT observations on July 16 (one day before the light curve presented here) revealed Cyg X–3 to be in a significantly brighter state in the IR (Fender 1995). This suggests a possible DC decline is superimposed upon the

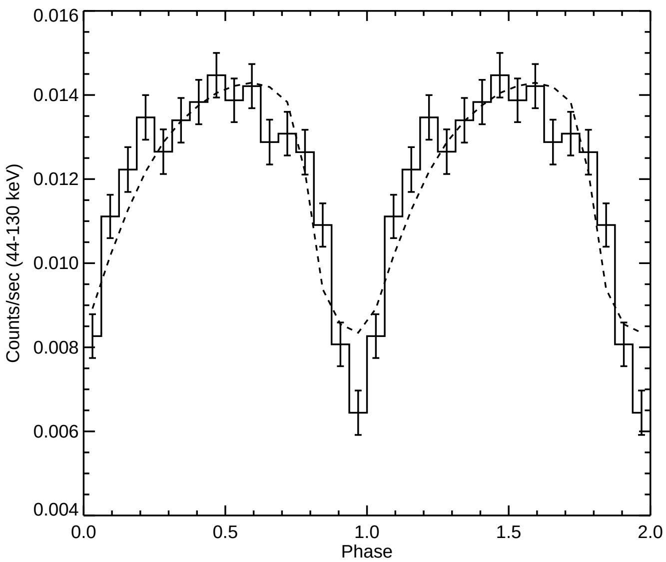

Fig. 3. OSSE average light curve, 1991–1994 with best-fit X-ray template (dashed line).

orbital light curve. This might affect both the light curve shape and the fitted phase.

Evolution of light curve shape with time is expected if the apparent orbital period change is due to apsidal motion. Some evidence for this was present in the earlier IR observations of Jones et al. (1994) where the light curve appeared more symmetric, and with a broader minimum, than seen in previous measurements.

The *combined* OSSE data offer some support for the hypothesis that the X-ray light curve shape has changed since the 1983–1985 EXOSAT observations. Figure 3 shows the average OSSE light curve from the seven observations from 1991 to 1994. This curve is inconsistent with the template light curve, also shown ($\chi^2 = 46.8$ for 13 dof, confidence level $= 1.0 \times 10^{-5}$). The light curve appears more symmetrical, with a somewhat narrower minimum. A transient change, over approximately one week, of the soft X-ray light curve from the template shape to a more symmetrical form has been observed by van der Klis & Bonnet-Bidaud (1981). However, such a change should have little effect on the average OSSE light curve, which combines ~ 65 days of observations.

It is possible that the light curve shape has not changed but is intrinsically different above 50 keV. This cannot be ruled out because there are no comparable hard X-ray light curves from earlier epochs. Also, there are no currently available soft X-ray light curves taken at the time of the OSSE data to make a contemporaneous comparison of light curve shapes in the different energy ranges. However, the independent evidence for light curve evolution in the infrared argues against this alternative.

5.3. Modulation

The modulation (light curve (max-min)/max) is a key test of source models. In these data we measured a modulation of $\sim 20\%$ for IR and $\sim 50\%$ for hard X-rays. The strong modulation in the hard X-rays is inconsistent with the extrapolation of the EXOSAT observations by Willingale, King, & Pounds (1985), which predict essentially no modulation at these energies. Strong hard X-ray modulation may be incompatible with their wind model of the Cyg X–3 light curve.

6. Summary and Conclusions

The current observations show some intriguing possible correlations between IR and hard X-ray behavior. In particular, the phases of flux minima are consistent at both wavelengths, and both show possible deviations from the historical soft X-ray light curve shape. However, strong variability in IR clouds the issue. To understand this highly variable source requires more coordinated observations, with better IR coverage over a longer period, coinciding with hard X-ray, soft X-ray, and radio measurements.

References

Bonnet-Bidaud, J. M., & Chardin, G. 1988, Phys. Reports, 170, 326

Elsner, R. F., Ghosh, P., Darbro, W., Weisskopf, M. C., Sutherland, P. G., & Grindlay, J. E. 1980, ApJ, 239, 335

Fender, R. P. 1995, PhD thesis, Open University, UK

Fender, R. P., & Bell Burnell, S. J. 1995, A&A, in press

Ghosh, P., Elsner, R. F., Weisskopf, M. C., & Sutherland, P. G. 1981, ApJ, 251, 230

Johnson, W. N., et al. 1993, ApJS, 86, 693

Jones, T. J., Gehrz, R. D., Kobulnicky, H. A., Molnar, L. A., & Howard, E. M. 1994, AJ, 108, 605

Kitamoto, S., Mizobuchi, S., Yamashita, K., & Nakamura, H. 1992, ApJ, 384, 263

Mason, K. O., Córdova, F. A., & White, N. E. 1986, ApJ, 309, 700

Matz, S. M., Grabelsky, D. A., Purcell, W. R., Ulmer, M. P., Johnson, W. N., Kinzer, R. L., Kurfess, J. D., & Strickman, M. S. 1994, in The Evolution of X-Ray Binaries (AIP Conf. Proc. 308), ed. S. S. Holt & C. S. Day (New York: AIP), 263

Milgrom, M., & Pines, D. 1978, ApJ, 220, 272

Molnar, L. A. 1988, ApJ, 331, L25

Pringle, J. E. 1974, Nature, 247, 21

van der Klis, M., & Bonnet-Bidaud, J. M. 1981, A&A, 95, L5

van der Klis, M., & Bonnet-Bidaud, J. M. 1989, A&A, 214, 203

van Kerkwijk, M. H., et al. 1992, Nature, 355, 703

White, N. E., & Holt, S. S. 1982, ApJ, 257, 318

Willingale, R., King, A. R., & Pounds, K. A. 1985, MNRAS, 215, 295

This article was processed by the author using Springer-Verlag LaTeX A&A style file *L-AA* version 3.